

Dear Editor,

We are submitting a revised version of the article entitled “Water-soluble iron emitted from vehicle exhaust is linked to primary speciated organic compounds” (manuscript acp-2019-RC1). We found the reviewers’ comments to be constructive and helpful during the revision process and see that our manuscript has been significantly improved as a result.

Please find the following documents in this submission: 1) A marked-up manuscript, 2) a clean manuscript, and 3) a point-by-point response to the Reviewer’s suggestions and concerns. Please note that Line numbers here refer to the clean revision.

Thank you for consideration of this manuscript.

Sincerely,

Brian J. Majestic, Ph.D.
Associate Professor
Chemistry & Biochemistry
University of Denver
Office: +1 303 871 2986
Fax: +1 303 871 2254

Reviewer 1

General:

This paper characterizes Fe solubility found in tailpipe emissions from different vehicle classes and proposes a mechanism involving Fenton chemistry with aromatic compounds to explain their results. This work is novel and of interest to the aerosol community. On another note, I found it refreshing to read an ACPD paper that was well-written yet concise. I recommend this paper for publication after addressing my minor comments.

Reply: We thank the Reviewer for their comments.

Major Comments:

1. The title is a bit awkward and overly complicated. I suggest that the authors simplify their title to something like “Water-soluble iron emitted from vehicle exhaust is linked to cyclic organic compounds”.

Reply: We agree that this would be clearer to the reader, so the title has been changed from “~~Water-soluble iron correlation to primary speciated organics in low-emitting vehicle exhaust~~” to “**Water-soluble iron emitted from vehicle exhaust is linked to primary speciated organic compounds**”

2. The rationale for targeting the IVOCs was not well-explained. I suggest a paragraph in the introduction briefly discussing different organics emitted from vehicles and what their possible role in Fe solubility may be.

Reply: The authors agree that a rationale for targeting IVOCs would be beneficial to the introduction. Line 81-89 refers to the research on organic species and solubilized iron. Line 89-92 was added to better explain the rationale for targeting IVOCs. Line 81-89 states “A third, broad, iron solubilization hypothesis

emphasizes an iron-organic interaction (Baba et al., 2015; Vile et al., 1987). For example, a significant increase in water-soluble iron is observed in the presence of oxalate and formate in ambient aerosols and in cloud droplets (Paris et al., 2011; Zhu et al., 1993). Other studies have suggested that the photolysis of polycyclic aromatic hydrocarbons leads to reduced iron, which may result in greater iron water solubility (Faiola et al., 2011; Haynes et al., 2019; Pehkonen et al., 1993; Zhu et al., 1993).”

Line 89-92: Vehicle exhaust contains many organic species including secondary organic aerosol (SOA) Single-ring aromatic compounds (C6-C9) PAHs, hopanes, steranes, alkanes, organic acids and intermediate volatility organic compound (IVOCs) which are longer chain organic species. (Cheung et al., 2010; Zhao et al., 2016)

Specific Comments:

Abstract:

1. Define EC and OC.

Reply: For clarification, Line 22-23 now reads “**elemental carbon (EC), organic carbon (OC)**”

2. Sentence on lines 21-24 needs to be rephrased. I found it confusing.

Reply: We thank the reviewer for this suggestion. To clarify for the reader, Line 23-26 has been divided in to two sentences and changed to “**Naphthalene and intermediate volatility organic compounds (IVOC) were quantified for a subset of vehicles. The IVOC quantified contained 12 to 18 carbons and were divided into three subgroups: aliphatic, single ring aromatic (SRA), and polar (material not classified as either aliphatic or SRA).**”

3. The end of the abstract should more clearly spell out the mechanism for the increased Fe solubility and include the role of Fenton chemistry.

Reply: To clarify for the reader, line 34-37 has been changed to “**These results suggest that the large driver in water-soluble iron from primary vehicle tail-pipe emissions is related to the organic composition of the PM. We hypothesize that, during the extraction process, specific components of the organic fraction of the PM are oxidized and chelate the iron into water**”

Introduction:

4. I suggest mentioning the different organics found in vehicle exhaust with attention to cyclic compounds and IVOCs. I also suggest mentioning how those compounds could affect Fe solubility to help establish the rationale for that aspect of your work.

Reply: 81-89 refers to the research on organic species and solubilized iron which led to the rationale to establish a relationship between water soluble iron and IVOCs. Line 81-89 states “A third, broad, iron solubilization hypothesis emphasizes an iron-organic interaction (Baba et al., 2015; Vile et al., 1987). For example, a significant increase in water-soluble iron is observed in the presence of oxalate and formate in ambient aerosols and in cloud droplets (Paris et al., 2011; Zhu et al., 1993). Even when compared to sulfuric acid, oxalic acid results in a greater increase in iron solubility because of the organic iron interaction (Chen and Grassian, 2013). Other studies have suggested that the photolysis of polycyclic aromatic hydrocarbons leads to reduced iron, which may result in greater iron water solubility (Faiola et al., 2011; Haynes and Majestic, 2019; Haynes et al., 2019; Pehkonen et al., 1993; Zhu et al., 1993).”

Line 89-92: Vehicle exhaust contains many organic species including secondary organic aerosol (SOA) Single-ring aromatic compounds (C6-C9) PAHs, hopanes, steranes, alkanes, organic acids and intermediate volatility organic compound (IVOCs) which are longer chain organic species. (Cheung et al., 2010; Zhao et al., 2016)

5. I encourage the authors to include and discuss the following papers relevant to this study in the introduction and the results section: [Chen and Grassian, 2013; Fu et al., 2012; Meskhidze et al., 2017]

Reply: We agree that these references are important for this topic, so the following lines have been added.

Line 57 “From these combustion sources, it has been shown that the species of iron differed greatly and had an impact in iron solubility (Fu et al., 2012).”

Line 84 “Even when compared to sulfuric acid, oxalic acid results in a greater increase in iron solubility because of the organic iron interaction (Chen and Grassian, 2013)”

Meskhidze et al., 2017, while important, was not added to the manuscript because a discussion of iron dissolved in seawater might confuse readers in understanding the context of this manuscript.

Methods:

1. Define FID

Reply: For clarity, Line 128-129 now reads **“by gas chromatography, with detection by a flame ionization detector (FID).”**

Results:

1. Figure S11 is important for showing that bulk organics and markers of inorganic acid processing (e.g., sulfate and nitrate) do not correlate with Fe and are not important for Fe solubility. I suggest showing at least these two aspects of your correlation analysis in the main manuscript and not in the SI.

Reply: We agree with this suggestion and a plot showing bulk organic carbon (OC) and sulfate is now Figure 3 in the manuscript and referenced in line 302 and 307.

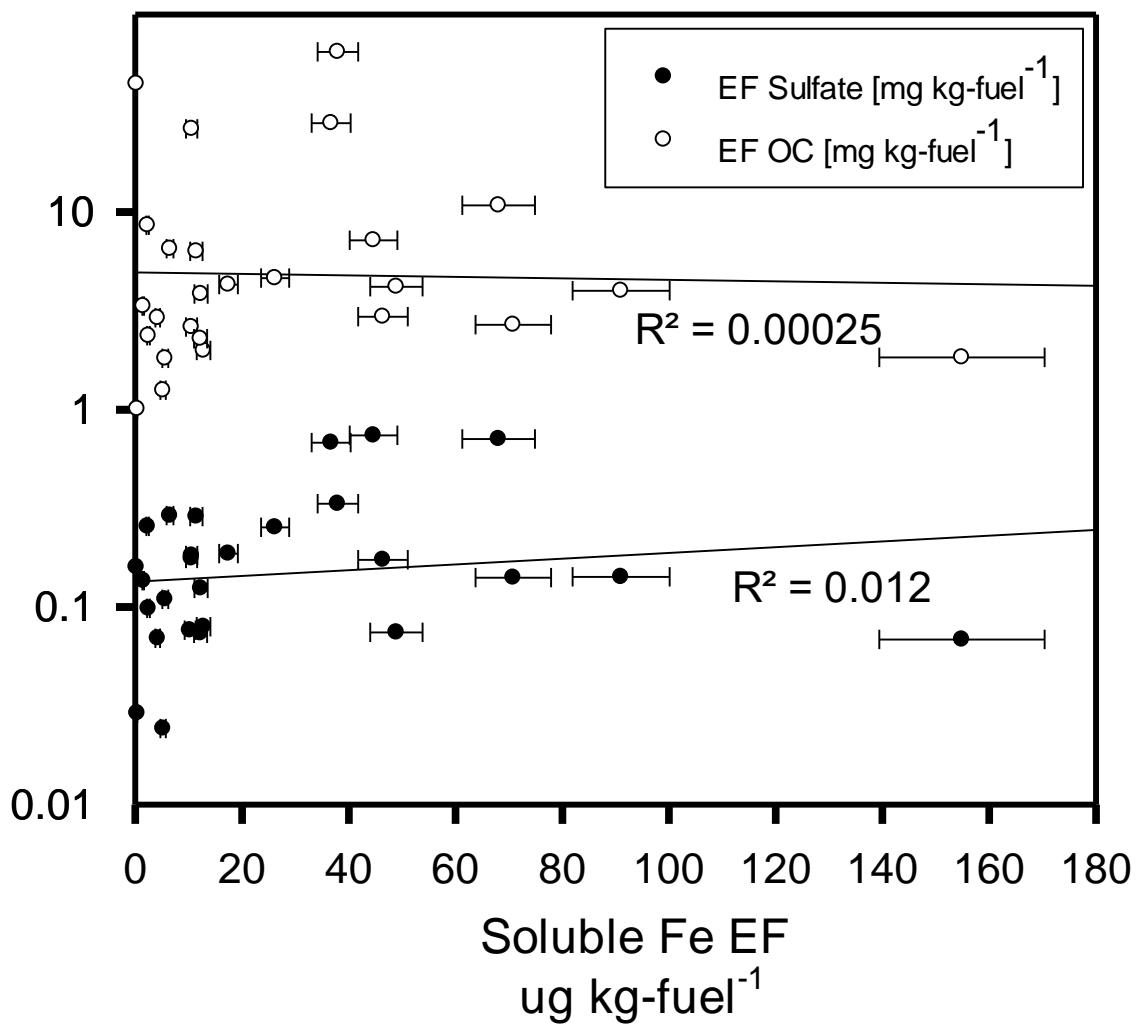


Figure 3: Linear correlation plots representing EF in mg kg-fuel-1 for sulfate and organic carbon (OC) in $\mu\text{g kg-fuel}^{-1}$ for water-soluble iron. Correlation lines and R2 values for all elements are shown.

2. Line 311: Define LFC.

Reply: LCF is defined in section 2.6 Line 191 in the methods “Least-square linear combination fitting (LCF) was subsequently performed in the range 7090 to 7365 eV to confirm iron valence and further identify the major mineral groups present.”

3. Line 324: provide some more rationale for why you targeted these specific organics.

Reply: To clarify for the reader, Line 340 was modified to **“leading to the investigation of organic species which resulted in a correlation to longer chain IVOC and naphthalene (Haynes and Majestic, 2019)“**

4. Lines 353-354: While these plots are compelling, the authors should provide a sentence or two with some explanation for the scatter in the data.

Reply: To address the scatter in the manuscript line 336 was added **“The variance of figure 4 could result from the fact that, in addition to the IVOCs, other factors also influence iron water solubility”**

Conclusions:

1. I suggest that the authors reiterate that Fe solubility was not related to inorganic acid processing. This is a very important point since many studies assume that sulfuric acid, in particular, is the most important acid that induces changes in Fe solubility.

Reply: We agree that this is one of the key points of the paper. Thus, we have changed line 410 to **“This study shows water-soluble iron is directly formed from vehicle exhaust and not correlated to sulfates”**

Reviewer 2

Summary:

The authors present a comprehensive study assessing the iron emitted by a collection of gasoline vehicles spanning a range of emissions certifications. This includes total iron and water-soluble iron as well as complementary analyses to determine the oxidation state of the iron. Interestingly, there is a trend between water-soluble iron emissions and intermediate-volatility organic compound (IVOC) emissions. Through a complementary laboratory study, the authors demonstrate that the iron may interact with some organic compounds, resulting in a transformation to water-soluble iron. Overall, this is a nice paper, and I recommend it for publication in *Atmospheric Chemistry and Physics*, pending adequate response to my comments and those from the other reviewers.

Reply: We thank the Reviewer for the kind words.

General Comments:

Some of the manuscript is unnecessarily repetitive. For example:

Lines 100-103, lines 115-118, and lines 126-127 are referring to particle sampling and analysis methods. Please combine to a single location within the document.

Reply: We thank the review for the suggestion to reduce the repetitiveness, lines 100-103, lines 115-118, and lines 126-127 are combined and line 110-116 now reads **“Emission samples were collected using a constant volume sampler from which a slipstream of dilute exhaust was drawn at a flow rate of 47 L min⁻¹. Particle phase emissions were collected using three sampling trains operated in parallel off of the end of the CVS dilution tunnel. Train 1 contained a Teflon filter (47 mm, Pall-Gelman, Teflo R2PJ047). Train 2 contained two quartz filters (47 mm, Pall-Gelman, Tissuquartz 2500 QAOUP) in series. Train 3 contained an acid-cleaned Teflon filter followed by a quartz filter (47 mm, Teflo, Pall Life Sciences, Ann Arbor, MI) and the flow rate was 0.5 L min⁻¹ through each Tenax tube.”**

Lines 115-118 and 126-127 were deleted.

Lines 129-131 and lines 142-144 both mention the use of a laminar flow hood for handling of samples. Please remove this redundancy.

Reply: To make the manuscript more concise, text in line 142 “~~and handled inside a polypropylene laminar flow hood (NuAire, Plymouth, MN)~~” was removed

In Figures 1, 2, and 4, please use “ μg ” rather than “ug”.

Reply: We thank the Reviewer for bringing this to our attention: We changed ug to μg in Figures 1, 2, and 4

Specific Comments:

Lines 61-63: Is the iron present in the gasoline itself, or does it leach from the vehicle components?

Reply: To avoid any misunderstanding, Line 65-69 changed to **“Iron is contained in many fuels which has pre-combusted concentrations ranging from 13-1000 $\mu\text{g L}^{-1}$ (Lee and Von Lehmden, 1973; Santos et al., 2011; Teixeira et al., 2007). Within the engine, computational models of combustion in engines suggest that iron emissions could also originate from the fuel injector nozzle inside the engine block (Liati et al., 2015).”**

Line 118-120: For a field campaign that occurred in 2014, I have a hard time believing that results were published in 2000. Please correct this reference.

Reply: We thank the Reviewer for catching this. We were using the methods, not the data. Thus, line 131-132 is changed to **“procedure for these data presented elsewhere”** from **“~~these data are presented elsewhere~~”**

Lines 156-159: How was 3% of the filters “measured exactly”? Was this using a filter punch that was precisely 3% of the area of the filters? Please clarify.

Reply: To clarify how the filters were cut Line 166-167 changed to **“~3% of the filters was measured and cut using a ceramic blade”**

Lines 178-182: I may have missed this definition, but what is “ μXRF ”? Does it differ from a typical X-ray fluorescence measurement?

Reply: The μ refers to the small spot size that the beam was able to fluoresce, thus line 188 has been changed to **“micro X-ray fluorescence (μXRF)”** and μXRF has been added to XRF in line 188 and 191 for consistency

Lines 235-241: It is a little unclear to me how the total iron emissions are defined. Is this the sum of the water-soluble iron from the water extractions described in Section 2.3 and the remaining iron that underwent the acid digestion in Section 2.4? Or was water-soluble iron determined from one filter and total iron determined from another filter? Please clarify.

Reply: Yes, the iron is summed from the water extractions described in Section 2.3 and the remaining iron that underwent the acid digestion in Section 2.4. Line 166-169 has been clarified to **“First ~3% (measured exactly) of the filters were cut and saved for X-ray absorption near edge structure (XANES) spectroscopy, then the water-soluble elements were extracted and, lastly the polymethylpentene ring was removed from the Teflon filters.”**

Lines 246-248: Why do the authors use the symbol from the periodic table for metals in previous sentence in this paragraph but not here?

Reply: We thank the Reviewer for bringing this to our attention. Elements in line 257 were changed to the names of the elements.

Lines 258-261: “Trace elements km⁻¹” and “per km emissions” are just distance-based emission factors (as opposed to the fuel-based emission factors that the authors have used). I recommend using “distance-based emission factors” in both of these lines.

Reply: We thank the reviewer for the clarification. “Trace elements km⁻¹” and “per km emissions” have been changed to “distance-based emission factors” in Lines 269-272 **“Table 2 compares the average exhaust PM composition and trace elements in distance-based emission factors in this study to literature values for other passenger vehicles, including one diesel and three gasoline exhaust studies. For all elements, the distance-based emission factors were greater in the diesel cohort, relative to the gasoline vehicles.”**

Figures 1 and 2: I’m wondering if it could be more informative to present the total iron emissions as, e.g., Figure 1a, and then have Figure 1b include box plots of the water-soluble iron fraction. This is just a thought that could potentially be more informative to drive home how much of the iron is actually water-soluble.

Reply: This is a great suggestion and we thank the reviewer. Below is the revised graph and the removed graph.

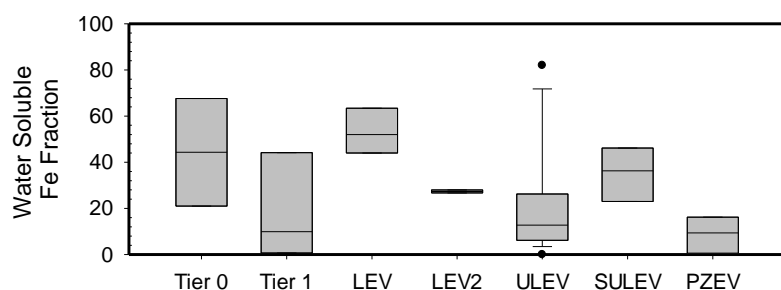


Figure 2: Water-soluble iron from the 32 vehicles tested reported in water-soluble iron fraction. The center black line represents the median value and the edges of the boxes represent the 25th and 75th percentiles while the whiskers are the 10th and 90th percentiles.

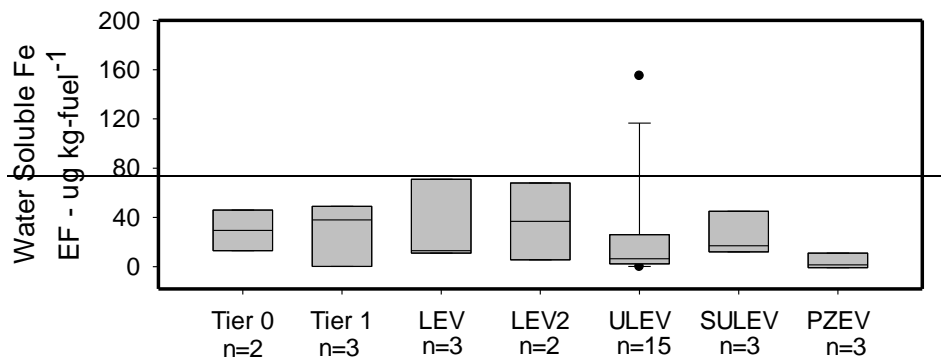


Figure 2: Water-soluble iron from the 32 vehicles tested reported in EF ($\mu\text{g kg-fuel}^{-1}$). The center black line represents the median value and the edges of the boxes represent the 25th- and 75th percentiles while the whiskers are the 10th- and 90th percentiles.

Lines 275-280: I have another thought on the presentation of results here. Given a lack of trend in total iron with emission certification, I'm curious if it would be worth exploring a trend in the ratio of total iron to particulate matter (PM) mass (e.g., $EF_{\text{Fe}}/EF_{\text{PM}}$). I suspect that the emissions of iron relative to total PM will increase, which could be an interesting result.

Reply: The authors agree that this could be useful, unfortunately overall PM mass wasn't measured as part of this study.

Lines 377-387: If I am understanding this correctly, it suggests that Fe(III) is emitted yet is rapidly converted to Fe(II). This may be worth stating explicitly.

Reply: Added to Line 406 to restate the above chemistry and clear up any confusion **“This overall process suggests that Fe(III) is emitted though car exhaust though interaction with water and organics undergoes a Fenton like reaction and converted to Fe(II) and the iron is chelated by the resulting oxidized organics.”**

Water-soluble iron emitted from vehicle exhaust is linked to primary speciated organic compounds

Joseph R. Salazar*, Benton T. Cartledge*, John P. Haynes*, Rachel York-Marini*, Allen L. Robinson[‡], Greg T. Drozd[€], Allen H. Goldstein[¥], Sirine C. Fakra[¢], Brian J. Majestic*

*University of Denver, Department of Chemistry and Biochemistry

[‡]Carnegie Mellon University, College of Engineering

[¥]University of California, Berkeley Department of Civil and Environmental Engineering

[€]Colby College Department of Chemistry

[¢]Advanced Light Source, Lawrence Berkeley National Laboratory, Berkeley, CA 94720

Correspondence to: Brian J. Majestic (brian.majestic@du.edu)

Abstract

Iron is the most abundant transition element in airborne PM, primarily existing as Fe(II) or Fe(III). Generally, the fraction of water-soluble iron is greater in urban areas compared to areas dominated by crustal emissions. To better understand the origin of water-soluble iron in urban areas, tail-pipe emission samples were collected from 32 vehicles with emission certifications of Tier 0, low emission vehicles (LEV I), tier two low emission vehicles (LEV II), ultralow emission vehicles (ULEV), superultra-low emission vehicles (SULEV), and partial-zero emission vehicles (PZEV). Components quantified included gases, inorganic ions, elemental carbon (EC), organic carbon (OC), total metals and water-soluble metals. Naphthalene and intermediate volatility organic compounds (IVOC) were quantified for a subset of vehicles. The IVOC quantified contained 12 to 18 carbons and were divided into three subgroups: aliphatic, single ring aromatic (SRA), and polar (material not classified as either aliphatic or SRA). Iron solubility in the tested vehicles ranged from 0 – 82% (average = 30%). X-ray absorption near edge structure (XANES) spectroscopy showed that Fe(III) was the primary oxidation state in 14 of the 16 tested vehicles, confirming that the presence of Fe(II) was not the main driver of water-soluble Fe. Correlation of water-soluble iron to sulfate was insignificant, as was correlation to every chemical component,

except to naphthalene and some C12- C18 IVOCs with R^2 values as high as 0.56. A controlled benchtop study confirmed that naphthalene, alone, increases iron solubility from soils by a factor of 5.5 and that oxidized naphthalene species are created in the extract solution. These results suggest that the large driver in water-soluble iron from primary vehicle tail-pipe emissions is related to the organic composition of the PM. We hypothesize that, during the extraction process, specific components of the organic fraction of the PM are oxidized and chelate the iron into water.

1. Introduction

Iron has been identified as a limiting nutrient for phytoplankton in approximately half of the world's oceans, with deposition from the atmosphere as the major source (Moore and Abbott, 2002; Sholkovitz et al., 2012). Phytoplankton is one of the controlling factors of fixed nitrogen in many parts of the oceans and, consequently, plays a major role in the ocean's biogeochemical cycles (Baker et al., 2006; Chen and Siefert, 2004; Kraemer, 2004; Shi et al., 2012; Tagliabue et al., 2017). Also, water-soluble iron fractions are linked to the creation of reactive oxygen species (ROS) in lung fluid and in environmental matrices through Fenton chemistry (Hamad et al., 2016). These ROS impart oxidative stress on the respiratory system, contributing to various health effects (Landreman et al., 2008; Park et al., 2006; Verma et al., 2014).

Annually, approximately 55 Tg of iron enters the atmosphere from crustal sources (Luo et al., 2008). Of this, 14-16 Tg are deposited into the ocean, impacting the marine life and influencing the ecosystems (Gao, 2003; Jickells et al., 2005). Typically, airborne iron from crustal sources ranges from 0.05-2% water-soluble of the total iron (Bonnet, 2004; Sholkovitz et al., 2012). Relative water-soluble iron in urban environments is higher, ranging from 2-50% of the total (Majestic et al., 2007; Sedwick et al., 2007; Sholkovitz et al., 2012). It is suggested that combustion sources including fossil fuel burning, incinerator use and biomass burning may be a large

contributor to the water-soluble iron fraction, contributing 0.66-1.07 Tg a⁻¹ of water-soluble iron and this iron has been correlated to anthropogenic sources (Chuang et al., 2005; Luo et al., 2008; Sholkovitz et al., 2009). From these combustion sources, it has been shown that the species of iron differed greatly and had an impact in iron solubility (Fu et al., 2012). Even though total iron emissions from combustion sources are small in comparison to crustal sources, the relative insolubility of crustal iron leads to the possibility that combustion sources contribute 20%-100% of water-soluble iron into the atmosphere (Luo et al., 2008; Sholkovitz et al., 2012).

Previous studies in tunnels and parking structures have reported iron ranging from five to approximately 3,500 ng m⁻³, revealing that brake wear, tire wear, resuspended road dust, and tail pipe emissions can be important sources of trace elements (Kuang et al., 2017; Lawrence et al., 2013; Li and Xiang, 2013; Lough et al., 2005; Park et al., 2006; Verma et al., 2014). Iron is contained in many fuels which has pre-combusted concentrations ranging from 13-1000 µg L⁻¹ (Lee and Von Lehmden, 1973; Santos et al., 2011; Teixeira et al., 2007). Within the engine, computational models of combustion in engines suggest that iron emissions could also originate from the fuel injector nozzle inside the engine block (Liati et al., 2015).

There are many different factors that may contribute to water-soluble iron and, as a result, several different hypotheses have been developed relating to how iron is solubilized in ambient atmospheres. First, correlation of ambient iron to sulfates in ambient aerosols suggest the possibility of iron solubilization (Desboeufs et al., 1999; Hand et al., 2004; Mackie et al., 2005; Oakes et al., 2012b). However, laboratory studies investigating the heterogeneous chemistry of iron have not shown any change in iron water-solubility, speciation, or oxidation state upon exposure to gaseous SO₂ (Cartledge et al., 2015; Luo et al., 2005; Majestic et al., 2007; Oakes et al., 2012a). A second hypothesis is that particle-bound iron oxidation state may control iron water

solubility. Thus far, the limited field studies have been unable to show that iron oxidation state is correlated to iron's resulting water solubility, as the majority of iron found in aerosol particles is in the less soluble Fe(III) oxidation state (Luo et al., 2005; Majestic et al., 2007; Oakes et al., 2012a). A third, broad, iron solubilization hypothesis emphasizes an iron-organic interaction (Baba et al., 2015; Vile et al., 1987). For example, a significant increase in water-soluble iron is observed in the presence of oxalate and formate in ambient aerosols and in cloud droplets (Paris et al., 2011; Zhu et al., 1993). Even when compared to sulfuric acid, oxalic acid results in a greater increase in iron solubility because of the organic iron interaction (Chen and Grassian, 2013). Other studies have suggested that the photolysis of polycyclic aromatic hydrocarbons leads to reduced iron, which may result in greater iron water solubility (Faiola et al., 2011; Haynes and Majestic, 2019; Haynes et al., 2019; Pehkonen et al., 1993; Zhu et al., 1993). Vehicle exhaust contains many organic species including secondary organic aerosol (SOA) Single-ring aromatic compounds (C6-C9) PAHs, hopanes, steranes, alkanes, organic acids and intermediate volatility organic compound (IVOCs) which are longer chain organic species (Cheung et al., 2010; Zhao et al., 2016).

In this study, we explore all three hypotheses (bulk ions, iron oxidation state, and organic speciation) in relation to iron solubility. Specifically, we examine the water-soluble iron emitted from 32 light duty gasoline vehicles with certifications of Tier 0, low emission vehicle (LEV I), tier two low emission vehicles (LEV II), ultralow emission vehicles (ULEV), superultra-low emission vehicles (SULEV), and partial-zero emission vehicles (PZEV). The total and water-soluble trace elements are compared to the ions, gaseous compounds, and organic emissions from the same vehicle set. Additionally, we acquired data on the emitted iron oxidation states on the exhaust particles. From this data set, real tail-pipe emission samples were explored to discover how various components of automobile exhaust affect the water solubility of iron.

2. Materials and Methods

2.1. Sample Collection

Exhaust samples from 32 gasoline vehicles were collected at the California Air Resources Board (CARB) Haagen-Smit laboratory over a six-week period. Standard emission test results from this campaign have been reported previously (Saliba et al., 2017). A description of the dynamometer, emission dilution system, and instrumentation used in the vehicle set up is provided elsewhere (May et al., 2014; Saliba et al., 2017). Briefly, each vehicle was tested on a dynamometer using the cold-start Unified California (UC) Drive Cycle or the hot start Modal Arterial Cycle 4. Emission samples were collected using a constant volume sampler from which a slipstream of dilute exhaust was drawn at a flow rate of 47 L min⁻¹. Particle phase emissions were collected using three sampling trains operated in parallel off of the end of the CVS dilution tunnel. Train 1 contained a Teflon filter (47 mm, Pall-Gelman, Teflo R2PJ047). Train 2 contained two quartz filters (47 mm, Pall-Gelman, Tissuquartz 2500 QAOUP) in series. Train 3 contained an acid-cleaned Teflon filter followed by a quartz filter (47 mm, Teflo, Pall Life Sciences, Ann Arbor, MI) and the flow rate was 0.5 L min⁻¹ through each Tenax tube. The particulate exhaust emissions were then collected on the pre-cleaned Teflon filters. The Teflon filters were stored in a freezer until extraction and analysis was performed. Filter holders were maintained at 47°C during sampling as per the CFR86 protocol.

The vehicles were recruited from private citizens, rental car agencies, or part of the Air Resource Board fleet. The vehicles tested were categorized by model years (1990-2014), vehicle type (passenger car and light-duty trucks), engine technologies (GDI and PFI), emission certification standards (Tier1 to SULEV), make, and model. All vehicles were tested using the same commercial gasoline fuel which had a 10 % ethanol blend and a carbon fraction of 0.82 (Saliba et al., 2017).

Gases (CO, CO₂, CH₄, NO, and NO₂) and total hydrocarbons (THC) were collected into heated Tedlar bags by UC Drive Cycles. Analysis of CO and CO₂ was measured by nondispersive infrared detectors (IRD-4000), CH₄ by gas chromatography, with detection by a flame ionization detector (FID), NO_x by chemiluminescence (CLD 4000) and THC by FID (Drozd et al., 2016; Saliba et al., 2017). The Teflon filter in Train 1 was analyzed by ion chromatography for water-soluble anions and cations and procedure for these data presented elsewhere (Hickox et al., 2000). Train 2 included two parallel sets of Tenax-TA sorbent tubes (Gerstel) downstream of the Teflon filter. The first set was 2 tubes connected in parallel. One of these tubes was used to collect emissions during the cold start phase of UC (the first five minutes, commonly referred to as bag 1). The other tube was used to sample emissions during the combined hot-running and hot start phases of the UC (bags 1 and 2). The second set of sorbent tubes was connected in series to collect emissions over the entire UC test. The Teflo filter in Train 3 was used for total and water-soluble trace element analysis and particle-bound iron oxidation state and is the focus of this study.

2.2. Materials Preparation

All vessel cleaning and analytical preparation for the trace elements was performed under a laminar flow hood with incoming air passing through a high efficiency particulate air (HEPA) filter. All water used was purified to 18.2 MΩ-cm (Milli-Q Thermo-Fisher Nanopore). Fifteen and 50 mL plastic centrifuge vials, Petri dishes (Fisher), Teflon forceps (Fisher), syringe (Fisher), nitro cellulose paper (Fisher), and syringe cases (Life Sciences Products) were prepped by an acid cleaning process. For the plastic centrifuge vials, Petri dishes, Teflon forceps, syringe, and syringe cases this involved 24-hour soaks in a 10% reagent grade nitric acid bath followed by 10% reagent grade hydrochloric bath then a 3% trace metal grade nitric acid (Fisher) resting bath with MQ rinses before, after and between each step. The nitro cellulose paper was cleaned by soaking in 2%

HCl for 24 hours then rinsing with MQ water. Then, 2% HCl and MQ water were pushed through the filter. Teflon beaker liners were cleaned by an acetone rinse, then an overnight bath of 100% HPLC-grade acetonitrile and a final overnight bath of 5% trace-metal grade nitric acid. 0.20 micron syringe filters (Whatman, Marlborough, MA) were prepared with 10% trace-metal grade hydrochloric acid, MQ water and 5% nitric acid rinse.

The 47 mm Teflon filters were cleaned by submerging them in 10% trace metal grade nitric acid and rinsing with MQ water. The filters were then stored in the acid cleaned Petri dishes and sealed with Teflon tape for storage.

2.3. Water-soluble metals sample preparations

Water-soluble elements were extracted for 2 hours from the Teflon filter on a shaker table in 10 mL of MQ water. The water extract was filtered with 2 μm pore size nitro cellulose filters. The Teflon filter and the nitro cellulose filters were saved for total metals digestion. The water-soluble element extract was acidified to 5% trace-metal grade nitric acid and 2.5% trace-metal grade hydrochloric acid to be analyzed by inductively coupled plasma mass spectrometry (ICP-MS, Agilent 7700).

2.4. Sample preparation for total elemental analysis

After the polymethylpentene ring was removed from the Teflon filters and ~3% of the filters were measured and cut using a ceramic blade and saved for X-ray absorption near edge structure (XANES) spectroscopy, then the water-soluble elements were extracted, and lastly the polymethylpentene ring was removed from the Teflon filters. The Teflon and the nitro cellulose filters for each sample were placed together into a microwave digestion vessel. To each digestion vessel, 750 μL of concentrated trace metal grade nitric acid, 250 μL of concentrated trace grade hydrochloric acid, 100 μL of concentrated trace grade hydrofluoric acid, and 100 μL of 30%

hydrogen peroxide was added. These samples were digested (Ethos EZ, Milestone Inc) according to the following a temperature program: 15-minute ramp to 200 °C, then held at 200 °C for 15 minutes, and a 60-minute cooling period.(Cartledge and Majestic, 2015) The samples were cooled to room temperature for 1 hour and the solution was diluted to 15 mL with MQ water and analyzed via ICP-MS.

2.5. Elemental analysis

Blank filters and standard reference materials (SRMs) were digested alongside the exhaust samples using the same digestion process described above. Three SRMs were used to address the recoveries of our digestion process: urban particulate matter (1648a, NIST), San Joaquin Soil (2709a, NIST), and Recycled Auto Catalyst (2556, NIST). The recoveries of the SRMs were between 80-120%. The elements analyzed included Na, Mg, Al, K, Ca, Ti, V, Cr, Mn, Fe, Co, Ni, Cu, Zn, As, Se, Rb, Sr, Mo, Rh, Pd, Ag, Cd, Sb, Cs, Ba, Ce, Pt, Pb, U. Indium (~1 ppb) was used as an internal standard and a He collision cell was used to remove isobaric interferences.

2.6. XANES Spectroscopy

X-ray absorption near-edge structure (XANES) and **micro X-ray fluorescence (μ XRF)** data for 16 vehicle exhaust samples were collected at the Advanced Light Source Microprobe beamline (10.3.2), Lawrence Berkeley National Laboratory, Berkeley, CA (Marcus et al., 2004). To locate iron spots on the filters, a broad **μ XRF** elemental map of each sample was acquired at 10 keV using 12 μ m by 12 μ m pixel size and 50 ms dwell time per pixel. μ XRF spectra were simultaneously recorded on each pixel of the map. Iron oxidation state and iron-bearing phases were investigated using iron K-edge extended XANES. The spectra were recorded in fluorescence mode by continuously scanning the Si (111) monochromator (Quick XAS mode) from 7011 to 7415 eV. The data were calibrated using an iron foil with first derivative set at 7110.75 eV (Kraft

et al., 1996). All data were recorded using a seven-element solid state Ge detector (Canberra, ON). The spectra were deadtime corrected, deglitched, calibrated, pre-edge background subtracted and post-edge normalized using a suite of LabVIEW custom programs available at the beamline (Marcus et al., 2008). To rapidly survey iron oxidation state, a valence scatter plot was generated from normalized XANES data using a custom Matlab code and a large database of iron standards (10.3.2 XAS database) (Marcus et al., 2008). Least-square linear combination fitting (LCF) was subsequently performed in the range 7090 to 7365 eV to confirm iron valence and further identify the major mineral groups present. The best fit was chosen based on 1) minimum normalized sum-square value ($NSS=100 \times [\sum(\mu_{\text{exp}} - \mu_{\text{fit}})^2 / \sum(\mu_{\text{exp}})^2]$), where the addition of a spectral component to the fit required a 10% or greater improvement in the NSS value, and 2) on the elements detected in the μ XRF spectrum recorded on each XANES spot. The uncertainty on the percentages of species present is estimated to be $\pm 10\%$.

2.7. Organic Speciation

A subset (10) of the 32 samples were quantified for IVOC using electron impact ionization with methods similar to that of Zhao et al., except adapted for GCxGC methods (Zhao et al., 2015, 2016). IVOC material was classified into three categories: aliphatic, single ring aromatic (SRA), and polar (Drozd et al., 2019). Classification within these three classes of compounds was determined by differences in second dimension retention time (polarity space) and by mass spectral characteristics in our GCxGC-MS analysis. All three classes of compounds were quantified by either compound specific calibration using known standards or relating total ion chromatogram (TIC) signals to calibration standards of similar volatility and polarity. In GCxGC, the TIC signal corresponds to a blob, or a region in volatility and polarity retention space. The GC-Image software package was used to create blobs from 2D chromatograms. Compounds were quantified by relating

their TIC signal to that of the nearest standard in terms of polarity and volatility. Volatility bins were defined that are evenly spaced with their center elution times corresponding to each *n*-alkane. TIC blobs were quantified using the calibration for the available standard of similar polarity in the same volatility bin.

2.8. Emission Factor Calculations

Emissions data are presented as fuel-based emission factors (EF). Emission factors are calculated as the amount of analyte emitted by mass per gram of fuel emitted.

$$EF_i(g\ g - fuel^{-1}) = \Delta m_i \frac{x_c(g)}{\Delta CO_2(g) + \Delta CO(g) + \Delta THC(g)}$$

ΔCO_2 , ΔCO , and ΔTHC are the background corrected carbon concentration of CO_2 , CO , and THC (Drozd et al., 2016; Goldstein et al., 2017), respectively. x_c is the fuel carbon mass fraction of 0.82. Δm_i is the blank subtracted concentrations of species *i*.

2.9. Naphthalene and Iron Benchtop Study

To better understand the production of soluble iron during the water extraction process, a benchtop study was performed using three varying forms of iron with naphthalene. The iron stock solutions/suspensions included: 1) standardized San Joaquin soil (NIST SRM 2709a) containing 25 ppm total iron (soluble + insoluble) iron to determine the effects of crustal iron, 2) iron(II) sulfate to a concentration of 25 ppm to examine the effect of a soluble iron(II) source, and 3) iron(III) sulfate to examine a source of soluble iron(III). In parallel, 100 mg of naphthalene crystals were added to 200 mL of MQ water. For the experiment, 99 mL of the naphthalene suspension and 1 mL of the iron suspension were added to Teflon liners (250 ppb iron total), which were inserted into a jacked glass beaker temperature controlled to 25 °C. After 16 hr of stirring, 2 mL were filtered (0.2 μm) and acidified to 5% nitric acid. Soluble iron released from the soil both in

the presence and absence of naphthalene was analyzed by ICP-MS. Chemical changes in naphthalene in the presence and absence of iron were monitored by HPLC.

3. Results and Discussion

3.1. Total and water-soluble element exhaust concentrations

Table 1:

Emissions of ions, organic species, gaseous species, and EC/OC from these tests have been published previously (Drozd et al., 2016, 2019; Goldstein et al., 2017; Saliba et al., 2017). In order to obtain a better understanding of the factors that influence iron solubility, we compare these with the total elements, trace elements, and iron oxidation state measurements. Generally, the elements with the highest EF are the lighter crustal elements Ca, Al, and Fe, with average EF 200, 100, and 80 $\mu\text{g kg-fuel}^{-1}$ (Table 1), respectively. Iron has the third highest average EF of all the elements and the highest of all transition elements, ranging from 0 – 200 $\mu\text{g Fe kg-fuel}^{-1}$. This is followed by three first row transition elements: Zn, Cu, and Ni with the respective average EF of 60, 20, and 5 $\mu\text{g kg-fuel}^{-1}$. Other notable elements include Rh, Pd and Pt, likely originating from the catalytic convertor, with the respective average EF of 0.05, 0.7, and 0.04 $\mu\text{g kg-fuel}^{-1}$. Toxic elements include Chromium, Lead, Molybdenum and Antimony with respective EF 5, 0.8, 5 and 0.2 $\mu\text{g kg-fuel}^{-1}$. A previous study has shown that various elements are enriched in used motor oil such as copper, zinc, manganese, iron and lead which could originate from engine wear (Majestic et al., 2009).

Table 1 also shows the EF for the water-soluble fraction of the trace elements. The water-soluble EF for iron ranges from 0-150 $\mu\text{g kg-fuel}^{-1}$; or 0-82% of the total. At 20 $\mu\text{g kg-fuel}^{-1}$, average water-soluble iron was the third largest EF of all elements. There were relatively high

emissions of a few other water-soluble elements such as Ca with an average EF of 200 $\mu\text{g kg-fuel}^{-1}$ and Zn with tailpipe emissions averaging 40 $\mu\text{g kg-fuel}^{-1}$.

Table 2:

Only a few studies report tailpipe emissions (i.e., dynamometer testing) of trace elements for diesel and gasoline-powered passenger cars and even fewer which have reported iron water

Table 2 compares the average exhaust PM composition and trace elements in distance-based emission factors in this study to literature values for other passenger vehicles, including one diesel and three gasoline exhaust studies. For all elements, the distance-based emission factors were greater in the diesel cohort, relative to the gasoline vehicles. Compared to previous studies, the trace elements emitted from older gasoline passenger vehicles resulted in an order of magnitude higher emissions for all elements, except for aluminum, which only showed a factor of ~2 increase in older vehicles (Table 2). Iron shows a large range in the three studies of gasoline vehicles, ranging from 8.3-280 $\mu\text{g km}^{-1}$, compared to the 0-62 $\mu\text{g km}^{-1}$ measured in this study.

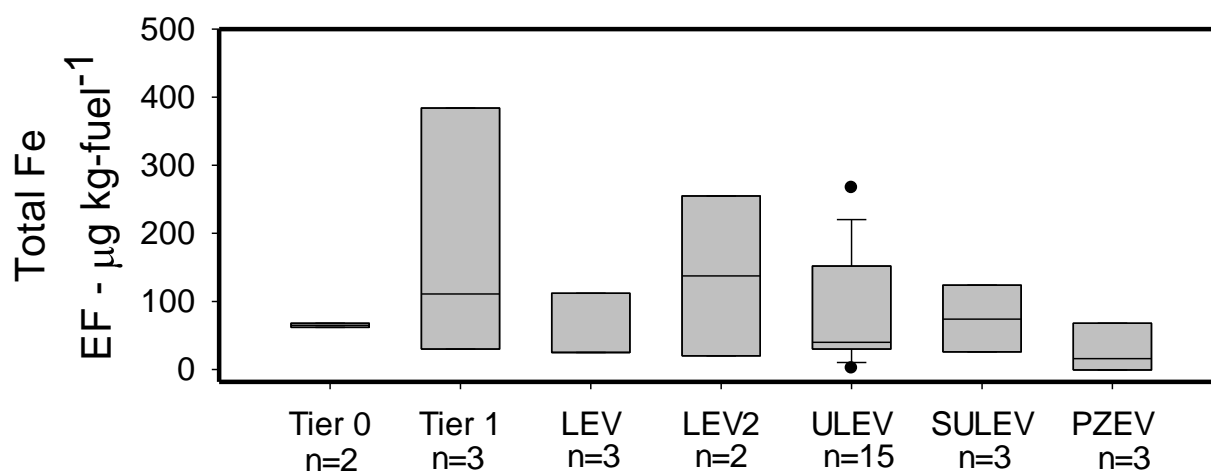


Figure 1: Total iron from the 32 vehicles tested reported in EF ($\mu\text{g kg-fuel}^{-1}$). The center black line represents the median value and the edges of the boxes represent the 25th and 75th percentiles while the whiskers extent are the 10th and 90th percentiles.

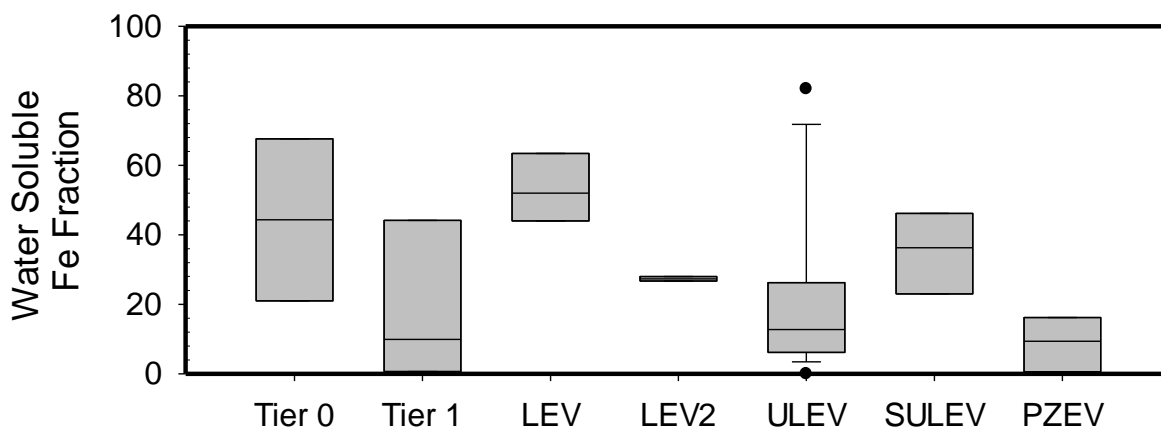


Figure 2: Water-soluble iron from the 32 vehicles tested reported in water-soluble iron fraction. The center black line represents the median value and the edges of the boxes represent the 25th and 75th percentiles while the whiskers are the 10th and 90th percentiles.

The large ranges in iron solubility of the previous studies led us to explore and compare the newer emission certification standard (Figure 1 and 2). Total iron did not trend strongly with emission certification standard, although, on average, total iron is less in the Tier 0 and LEV vehicles. Water-soluble iron shows a small average decrease of approximately $5 \mu\text{g kg-fuel}^{-1}$ between ULEV and SULEV vehicles, and a further average decrease for the PZEV vehicles of $3.9 \mu\text{g kg-fuel}^{-1}$.

3.2. Iron correlations with bulk exhaust components and iron oxidation state

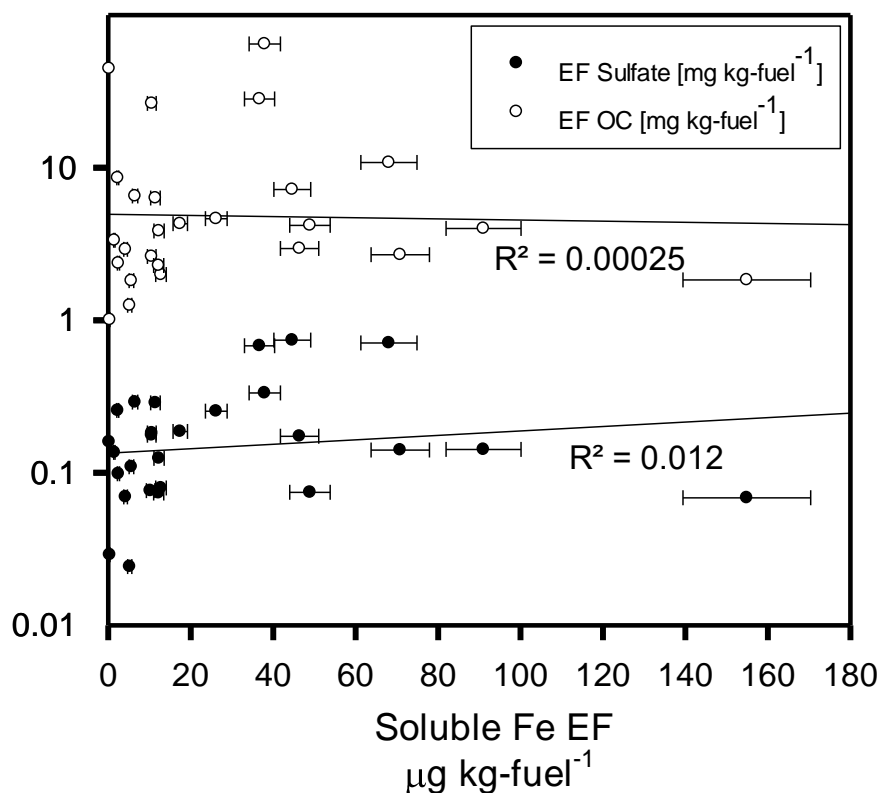


Figure 3: Linear correlation plots representing EF in mg kg-fuel^{-1} for sulfate and organic carbon (OC) in $\mu\text{g kg-fuel}^{-1}$ for water-soluble iron. Correlation lines and R^2 values for all elements are shown.

To explore what factors and if any exhaust components are associated with the presence of water-soluble iron, linear regression analyses were used to compare soluble iron to different chemical species in the exhaust. Solubility from the direct exhaust was explored by comparing the EFs of both sulfate and nitrate to iron, and water-soluble iron was not correlated to either of these species (SI1 and Figure 3). The EFs for water-soluble iron and CO_2 showed no correlation, suggesting that overall fuel use was not an important factor for water-soluble iron production (SI1).

Total iron was correlated to the water-soluble iron indicating the total amount of iron may have an impact on soluble iron (SI2). Finally, to evaluate if water-soluble iron and overall particulate carbon relate, the EFs for elemental carbon (EC) and organic carbon (OC) were compared to that of soluble iron and, again, no correlation was observed (SI1 and Figure 3).

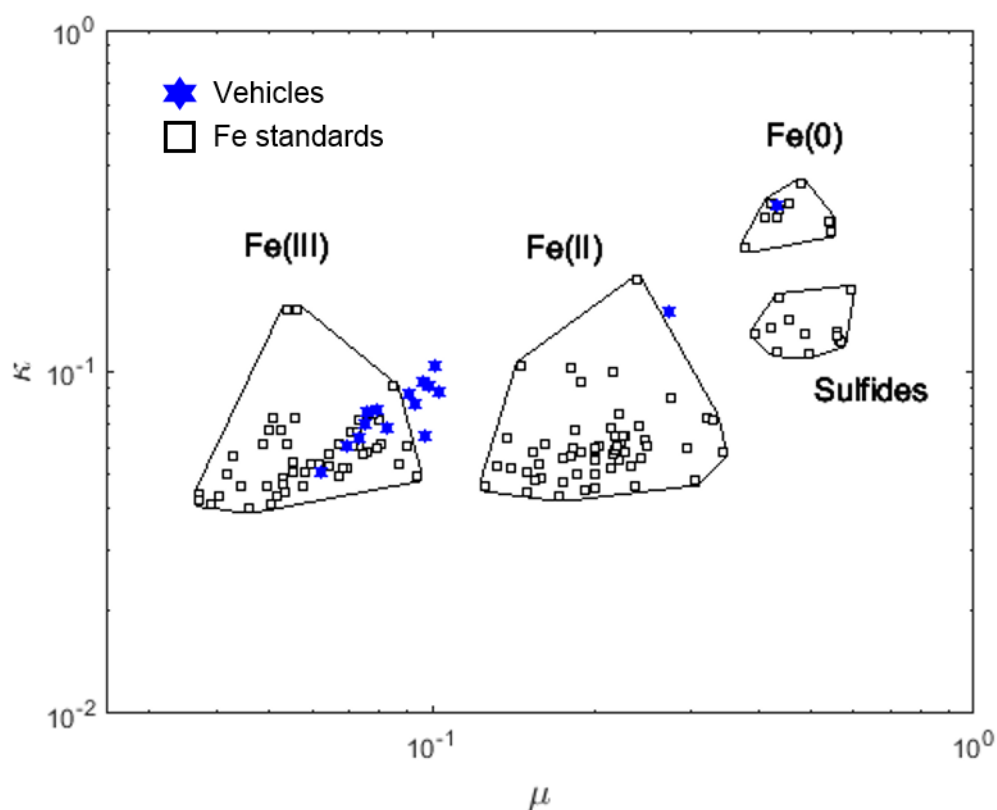


Figure 4: Fe valence scatter plot generated from Fe K-edge XANES data where κ and μ are normalized absorbance values at 7113 eV and 7117.5 eV respectively. Empty black squares represent Fe standards of known valence while blue-filled stars represent vehicle exhaust samples.

As no correlation between water-soluble iron and bulk chemical species was observed (SI1 and SI3), the importance of the particle-bound iron oxidation state was investigated. Since Fe(II) is known to be more soluble than Fe(III), the expectation was that exhaust samples having a large

Fe(II) character would have a greater iron solubility, relative to those containing Fe(III) or to Fe(0) (Stumm and Morgan, 1996). Figure 3 presents a scatter plot of the iron valence in 16 of the exhaust samples, compared with iron-bearing standards of known valence. This valence plot is generated from iron K-edge XANES data where parameters κ and μ are defined as normalized absorbance values at 7113 eV and 7117.5 eV, respectively. We observe that the exhaust-iron is primarily in the Fe(III) oxidation state, except for two vehicles: sample 11, dominated by Fe(0) and sample 15, containing a combination of Fe(0) and Fe(III) (SI4). Sample 11 is an extreme case, having 0 % iron solubility and highly elevated amount of EC at 305 $\mu\text{g kg-fuel}^{-1}$ (study average = 78 $\mu\text{g kg-fuel}^{-1}$). The presence of Fe(0) is consistent with high EC, as both observations suggest a lack of oxidation during the combustion and emission process. While the valence plot (Figure 3) put sample 15 as mostly Fe(II), the LCF actually showed that it was a mixture of Fe(0) and Fe(III). And, this sample contained only 10% water-soluble iron, less than the cohort average. The study-wide solid phase iron oxidation state is primarily Fe(III) or mixed oxidation state (Fe(III) and Fe(0)) (see Figure 3), averaging about 30% water-soluble iron, well above the crustal background. LCF XANES fitting (SI4) showed Fe(III) oxides and oxyhydroxides as the dominant group, followed by Fe(III) sulfates and iron silicates (SI4). Hematite ($\alpha\text{-Fe}_2\text{O}_3$) and maghemite ($\gamma\text{-Fe}_2\text{O}_3$) were the most consistently detected Fe(III) oxides. Iron was detected in all samples, with Zn, Cr and Cu the main other elements detected in nearly all samples (detection of low-Z elements below sulfur or high-Z elements above zinc was not possible in our experimental conditions). Overall, these results strongly suggest that the main driver of water-soluble iron is not associated with the particle-bound iron oxidation state. Further investigation for the LCF XANES fitting showed that 34% of iron speciated was Fe(III)-oxyhydroxides associated with organic material leading to the

investigation of organic species which resulted in a correlation to longer chain IVOC and naphthalene (SI6) (Haynes and Majestic, 2019).

3.3. Iron solubility and speciated organics

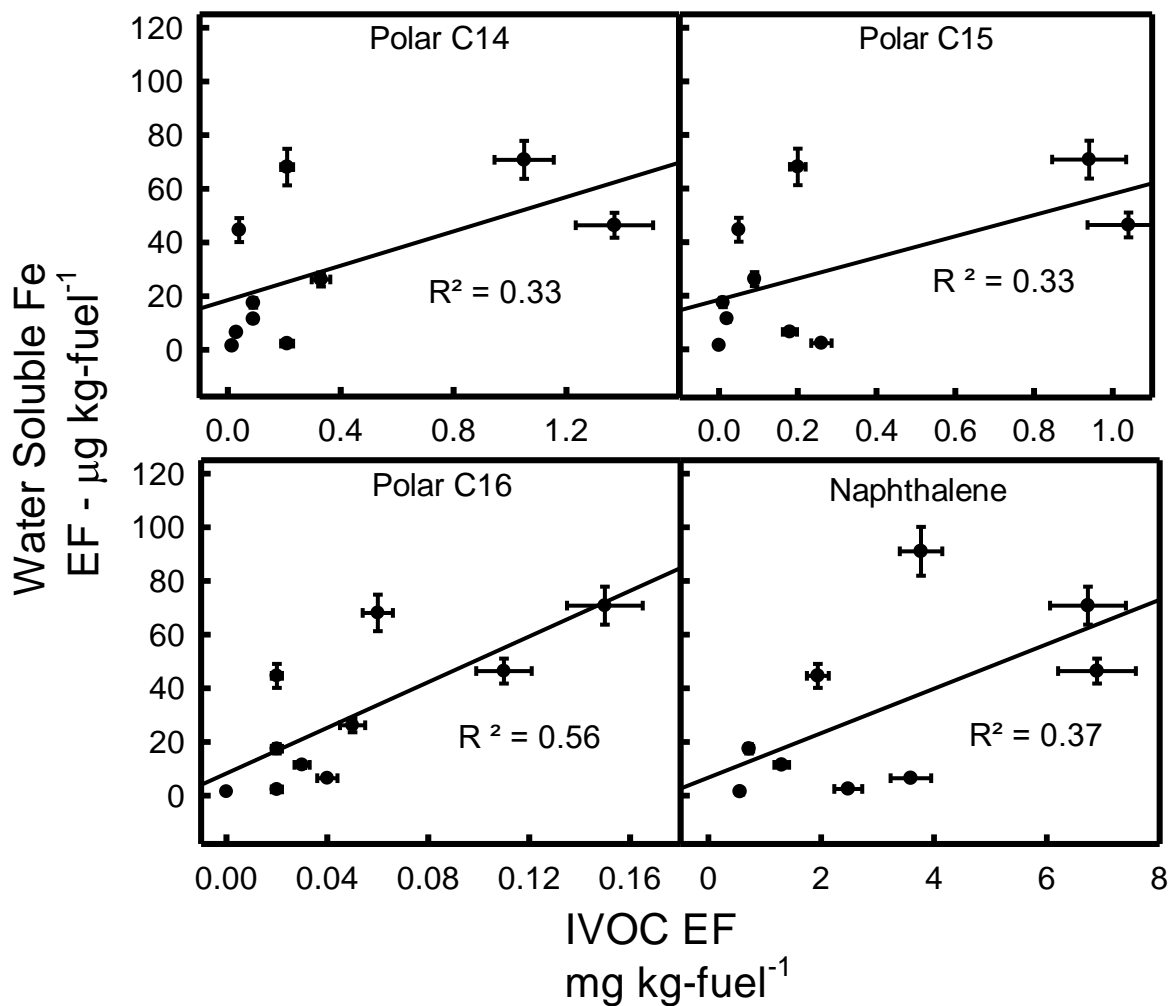


Figure 5: Scatter plots of water-soluble iron versus the sum of IVOCs reported in EF (g kg-fuel^{-1}).

Finally, the relationship between water-soluble iron and speciated organics, specifically naphthalene and IVOCs, was examined. In contrast with all other measured parameters, Figure 4 shows relatively strong correlations between water-soluble iron and some of the IVOC species. Figure 4 presents the classifications which have the strongest correlation with water-soluble iron.

Water-soluble iron relationships with other IVOCs can be found in the supplementary information (SI8). The correlation to water-soluble iron is highest for IVOC-polar species with 16 carbons ($R^2 = 0.56$). The variance of figure 4 could result from the fact that, in addition to the IVOCs, other factors also influence iron water solubility.

As water-soluble iron trends well with naphthalene and polar-IVOCs, but not with bulk EC or OC, it is highly suggestive that iron solubility from the direct emission samples is primarily dependent on interactions with the species of carbon present in the particles during the extraction process. To better understand these interactions, a preliminary laboratory study was conducted to explore both i) the effect of these organic compounds on iron solubility and ii) the effect of soluble iron on the oxidation of organic compounds during the extraction process. Specifically, when naphthalene was added to an insoluble iron source (a soil), iron solubility increased from 0.8 to 4.2 % of the total, or by a factor of ~5.5, showing that the addition of naphthalene, alone, can have a significant effect on iron water solubility and that this effect likely is important during the extraction process.

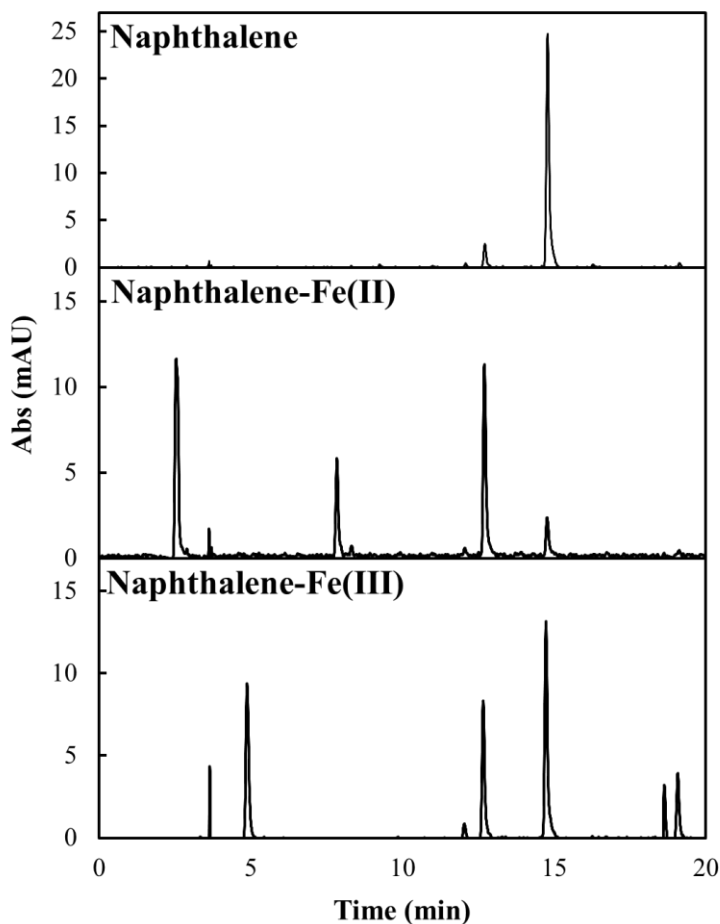


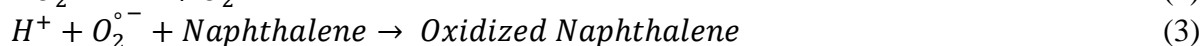
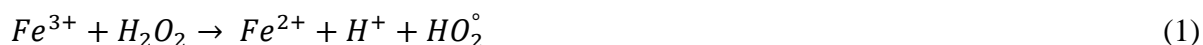
Figure 6: HPLC of resulting reaction between naphthalene and water-soluble iron. Phthalic acid at 12.5 minutes, phthalic anhydride at 7.5 minutes, naphthol at 15 minutes and naphthalene at 20 minutes. The column uses a C18 stationary phase on beads with 80Å pore size.

Lacking oxidized functional groups, naphthalene was not expected to chelate iron or to, otherwise, have the ability to increase iron solubility. Thus, we investigated what compounds are formed from naphthalene during these extractions. Figure 5 shows the new oxidized products formed from naphthalene during the water extraction. In the presence of soluble iron, HPLC retention time analysis shows the presence of phthalic acid (12.5 minutes), phthalic anhydride (7.5 minutes), and naphthol (15 minutes). The peaks at and below 5 min were not identified but, based

on the retention times, these are thought to be low molecular mass, highly polar organic products and is consistent with other studies (Haynes et al., 2019)

3.4. Iron-carbon interactions

There are at least two methods in which organic compounds can lead to increased iron solubility: a) reduction of Fe(III) to Fe(II) or b) bringing soluble iron into solution via chelation. The first one is generally achieved by photochemistry (Pehkonen et al., 1993), which is not directly applicable to this study. The second, chelation, generally requires oxidized functional groups as shown in Figure 5. The extent of the ability for phthalic acid (a dicarboxylic acid) to chelate iron has not been reported, however, it is known that similar molecular mass organic diacids have significant ability to chelate iron, thus pulling it into solution (Paris and Desboeufs, 2013). Here, we suggest that the observed correlations between IVOC/naphthalene and water-soluble iron can be best explained with Fenton reactions, resulting in propagation of radical reactions (Pehkonen et al., 1993). As shown from the Fe XANES valence plot, the iron is predominately Fe(III) (Figure 4). In addition to the Fe(III), it has been shown that H₂O₂ forms in PM_{2.5} water extracts and it been speculated that this formation is from various transition metals and/or quinones found in PM_{2.5} (Wang et al., 2012).



In the presence of H₂O₂, Fe(III) is known to undergo reaction (1) (Neyens and Baeyens, 2003; Pignatello et al., 2006), resulting in the formation of Fe(II) and HO₂ (Pignatello et al., 2006; Rubio-Clemente et al., 2014), which degrades into superoxide, O₂⁻, and H⁺ (2). Superoxide has the ability to oxidize organic compounds, particularly aromatic structures (3) (Lair et al., 2008). The resulting structures of these oxidized compounds typically have two oxygen atoms, which could

be arranged in various functional groups (Lair et al., 2008; Rubio-Clemente et al., 2014), also observed from the HPLC chromatograms. Oxidized single ring aromatic structures have a strong affinity to iron and have the ability chelate iron into aqueous solution (Haynes and Majestic, 2019; Hosseini and Madarshahian, 2009). Based on the laboratory studies of naphthalene and soluble-iron presented here, naphthalene and/or IVOC oxidation during the extraction process is the most likely path towards increased iron solubility in primary tailpipe emissions. This overall process suggests that Fe(III) is emitted through car exhaust through interaction with water and organics undergoes a Fenton like reaction and converted to Fe(II) and the iron is chelated by the resulting oxidized organics.

4. Conclusions

This study shows water-soluble iron is directly formed from vehicle exhaust and not correlated to sulfates. The results show that iron is solubilized in water by specific organic compounds present in automobile exhaust, and that soluble iron is not necessarily dictated by the overall OC content. Thus, the implication is that anthropogenic water-soluble iron is a result of chelation from specific organic compounds, likely their eventual aqueous reaction products. Although the mechanism of these aqueous transformations were not directly measured in this study, based on Fenton chemistry, the primary compounds are expected to be oxidized versions of naphthalene and/or IVOCs (Ledakowicz et al., 1999). Since these oxidation reactions occur fairly quickly (i.e., during the water extraction), further studies are of interest to better understand how these organic compounds interact with iron as it enters atmospheric waters and, also, the photochemical interactions between iron and organics.

Acknowledgements

The authors thank the excellent and dedicated personnel at the California Air Resources Board, especially at the Haagen–Smit Laboratory. This study was funded by National Science Foundation grant numbers 1342599 and 1549166. This research used resources of the Advanced Light Source, which is a DOE Office of Science User Facility under contract no. DE-AC02-05CH11231. Financial support was provided by the California Air Resources Board (Contract #12-318). The California Air Resources Board also provided substantial in-kind support for vehicle procurement, testing, and emissions characterization.

Author contribution

The sample collection scheme was designed by Allen L. Robinson, Allen H. Goldstein and Brian J. Majestic. Samples were collected by Benton T. Cartledge and Greg T. Drozd. Organic speciation was performed by Greg T. Drozd. Trace elements were quantified by Joseph R. Salazar. Iron speciation was performed by Joseph R. Salazar, Rachel York-Marini and Brian J. Majestic, with the interpretation effort led by Sirine C. Fakra. Bench-top naphthene experiments were performed by John P. Haynes. Data integration was performed by Joseph R. Salazar. The manuscript was prepared by Joseph R. Salazar and Brian J. Majestic.

References

Baba, Y., Yatagai, T., Harada, T. and Kawase, Y.: Hydroxyl radical generation in the photo-fenton process: Effects of carboxylic acids on iron redox cycling, *Chem. Eng. J.*, 277, 229–241, doi:10.1016/j.cej.2015.04.103, 2015.

Baker, A. R., Jickells, T. D., Witt, M. and Linge, K. L.: Trends in the solubility of iron, aluminium, manganese and phosphorus in aerosol collected over the Atlantic Ocean, *Mar. Chem.*, 98(1), 43–58, doi:10.1016/j.marchem.2005.06.004, 2006.

Bonnet, S.: Dissolution of atmospheric iron in seawater, *Geophys. Res. Lett.*, 31(3), L03303, doi:10.1029/2003GL018423, 2004.

Cartledge, B. T. and Majestic, B. J.: Metal concentrations and soluble iron speciation, *Atmos. Pollut. Res.*, (6), 495–505, 2015.

Cartledge, B. T., Marcotte, A. R., Herckes, P., Anbar, A. D. and Majestic, B. J.: The Impact of Particle Size, Relative Humidity, and Sulfur Dioxide on Iron Solubility in Simulated Atmospheric Marine Aerosols, *Environ. Sci. Technol.*, 49(12), 7179–7187, doi:10.1021/acs.est.5b02452, 2015.

Chen, Y. and Siefert, R. L.: Seasonal and spatial distributions and dry deposition fluxes of atmospheric total and labile iron over the tropical and subtropical North Atlantic Ocean, *J. Geophys. Res. D Atmos.*, 109(9), doi:10.1029/2003JD003958, 2004.

Cheung, K. L., Ntziachristos, L., Tzamkiozis, T., Schauer, J. J., Samaras, Z., Moore, K. F. and Sioutas, C.: Emissions of particulate trace elements, metals and organic species from gasoline, diesel, and biodiesel passenger vehicles and their relation to oxidative potential, *Aerosol Sci. Technol.*, 44(7), 500–513, doi:10.1080/02786821003758294, 2010.

Chuang, P. Y., Duvall, R. M., Shafer, M. M. and Schauer, J. J.: The origin of water soluble particulate iron in the Asian atmospheric outflow, *Geophys. Res. Lett.*, 32(7), 1–4, doi:10.1029/2004GL021946, 2005.

Desboeufs, K. V, Losno, R. and Cholbi, S.: The pH-dependent dissolution of wind-transported, , 104, 1999.

Drozd, G. T., Zhao, Y., Saliba, G., Frodin, B., Maddox, C., Weber, R. J., Chang, M. C. O., Maldonado, H., Sardar, S., Robinson, A. L. and Goldstein, A. H.: Time Resolved Measurements of Speciated Tailpipe Emissions from Motor Vehicles: Trends with Emission Control Technology, Cold Start Effects, and Speciation, *Environ. Sci. Technol.*, 50(24), 13592–13599, doi:10.1021/acs.est.6b04513, 2016.

Drozd, G. T., Zhao, Y., Saliba, G., Frodie, B., Maddox, C., Chang, M.-C. O., Maldonado, H., Sardar, S., Weber, R. J., Robinson, A. L. and Goldstein, A. H.: Detailed Speciation of Intermediate Volatility and Semivolatile Organic Compound Emissions from Gasoline Vehicles: Effects of Cold-Starts and Implications for Secondary Organic Aerosol Formation., *Environ. Sci. Technol.*, 53(3), 1706–1714, 2019.

Faiola, C., Johansen, A. M., Rybka, S., Nieber, A., Thomas, C., Bryner, S., Johnston, J., Engelhard, M., Nachimuthu, P. and Owens, K. S.: Ultrafine particulate ferrous iron and anthracene associations with mitochondrial dysfunction, *Aerosol Sci. Technol.*, 45(9), 1109–1122, doi:10.1080/02786826.2011.581255, 2011.

Gao, Y.: Aeolian iron input to the ocean through precipitation scavenging: A modeling perspective and its implication for natural iron fertilization in the ocean, *J. Geophys. Res.*, 108(D7), 4221, doi:10.1029/2002JD002420, 2003.

Goldstein, A., Robinson, A., Kroll, J., Drozd, G., Zhao, Y., Saliba, G., Saleh, R. and Presto, A.: Investigating Semi-Volatile Organic Compound Emissions from Light-Duty Vehicles., 2017.

Hamad, S. H., Schauer, J. J., Antkiewicz, D. S., Shafer, M. M. and Kadhim, A. K. H.: ROS production and gene expression in alveolar macrophages exposed to PM_{2.5} from Baghdad, Iraq:

Seasonal trends and impact of chemical composition, *Sci. Total Environ.*, 543, 739–745, doi:10.1016/j.scitotenv.2015.11.065, 2016.

Hand, J. L., Mahowald, N. M., Chen, Y., Siefert, R. L., Luo, C., Subramaniam, A. and Fung, I.: Estimates of atmospheric-processed soluble iron from observations and a global mineral aerosol model: Biogeochemical implications, *J. Geophys. Res. D Atmos.*, 109(17), 1–21, doi:10.1029/2004JD004574, 2004.

Haynes, J. and Majestic, B.: Role of polycyclic aromatic hydrocarbons on the photo-catalyzed solubilization of simulated soil-bound atmospheric iron, *Atmos. Pollut. Res.*, doi:https://doi.org/10.1016/j.apr.2019.12.007, 2019.

Haynes, J. P., Miller, K. E. and Majestic, B. J.: Investigation into Photoinduced Auto-Oxidation of Polycyclic 2 Aromatic Hydrocarbons Resulting in Brown Carbon Production, *Environ. Sci. Technol.*, 53(3), 10.1021/acs.est.8b05704, doi:10.1021/acs.est.8b05704, 2019.

Hickox, W. H., Werner, B. and Gaffney, P.: Air Resources Board, , (MId), 1–6 [online] Available from: http://www.arb.ca.gov/ei/see/memo_ag_emission_factors.pdf, 2000.

Hosseini, M. S. and Madarshahian, S.: Investigation of charge transfer complex formation between Fe(III) and 2,6-Dihydroxy benzoic acid and its applications for spectrophotometric determination of iron in aqueous media, *E-Journal Chem.*, 6(4), 985–992, doi:10.1155/2009/417303, 2009.

Jickells, T. D., An, Z. S., Andersen, K. K., Baker, a R., Bergametti, G., Brooks, N., Cao, J. J., Boyd, P. W., Duce, R. a, Hunter, K. a, Kawahata, H., Kubilay, N., LaRoche, J., Liss, P. S., Mahowald, N., Prospero, J. M., Ridgwell, a J., Tegen, I. and Torres, R.: Global iron connections between desert dust, ocean biogeochemistry, and climate., *Science*, 308(5718), 67–71, doi:10.1126/science.1105959, 2005.

Kraemer, S. M.: Iron oxide dissolution and solubility in the presence of siderophores, *Aquat. Sci.*,

66(1), 3–18, doi:10.1007/s00027-003-0690-5, 2004.

Kraft, S., Stümpel, J. and Becker, P.: High resolution x-ray absorption spectroscopy with absolute energy calibration for the determination of absorption edge energies, *Rev. Sci. Instrum.*, 67, 681, 1996.

Kuang, X. M., Scott, J. A., da Rocha, G. O., Betha, R., Price, D. J., Russell, L. M., Cocker, D. R. and Paulson, S. E.: Hydroxyl radical formation and soluble trace metal content in particulate matter from renewable diesel and ultra low sulfur diesel in at-sea operations of a research vessel, *Aerosol Sci. Technol.*, 51(2), 147–158, doi:10.1080/02786826.2016.1271938, 2017.

Lair, A., Ferronato, C., Chovelon, J. M. and Herrmann, J. M.: Naphthalene degradation in water by heterogeneous photocatalysis: An investigation of the influence of inorganic anions, *J. Photochem. Photobiol. A Chem.*, 193(2–3), 193–203, doi:10.1016/j.jphotochem.2007.06.025, 2008.

Landreman, A. P., Shafer, M. M., Hemming, J. C., Hannigan, M. P. and Schauer, J. J.: A Macrophage-Based Method for the Assessment of the Reactive Oxygen Species (ROS) Activity of Atmospheric Particulate Matter (PM) and Application to Routine (Daily-24 h) Aerosol Monitoring Studies, *Aerosol Sci. Technol.*, 42(11), 946–957, doi:10.1080/02786820802363819, 2008.

Lawrence, S., Sokhi, R., Ravindra, K., Mao, H., Prain, H. D. and Bull, I. D.: Source apportionment of traffic emissions of particulate matter using tunnel measurements, *Atmos. Environ.*, 77, 548–557, doi:10.1016/j.atmosenv.2013.03.040, 2013.

Ledakowicz, S., Miller, J. S. and Olejnik, D.: Oxidation of PAHs in water solutions by ultraviolet radiation combined with hydrogen peroxide, *Int. J. Photoenergy*, 1(1), 1–6, doi:10.1155/S1110662X99000100, 1999.

Li, Y. and Xiang, R.: Particulate pollution in an underground car park in Wuhan, China, *Particuology*, 11(1), 94–98, doi:10.1016/j.partic.2012.06.010, 2013.

Lough, G. C., Schauer, J. J., Park, J. S., Shafer, M. M., Deminter, J. T. and Weinstein, J. P.: Emissions of metals associated with motor vehicle roadways, *Environ. Sci. Technol.*, 39(3), 826–836, doi:10.1021/es048715f, 2005.

Luo, C., Mahowald, N. M., Meskhidze, N., Chen, Y., Siefert, R. L., Baker, A. R. and Johansen, A. M.: Estimation of iron solubility from observations and a global aerosol model, *J. Geophys. Res. Atmos.*, 110(23), 1–23, doi:10.1029/2005JD006059, 2005.

Luo, C., Mahowald, N., Bond, T., Chuang, P. Y., Artaxo, P., Siefert, R., Chen, Y. and Schauer, J.: Combustion iron distribution and deposition, *Global Biogeochem. Cycles*, 22, doi:10.1029/2007GB002964, 2008.

Mackie, D. S., Boyd, P. W., Hunter, K. A. and McTainsh, G. H.: Simulating the cloud processing of iron in Australian dust: pH and dust concentration, *Geophys. Res. Lett.*, 32(6), 1–4, doi:10.1029/2004GL022122, 2005.

Majestic, B. J., Schauer, J. J. and Shafer, M. M.: Application of synchrotron radiation for measurement of iron red-ox speciation in atmospherically processed aerosols, *Atmos. Chem. Phys.* *Atmos. Chem. Phys.*, 7(Iii), 2475–2487, doi:10.5194/acpd-7-1357-2007, 2007.

Majestic, B. J., Anbar, A. D. and Herckes, P.: Elemental and iron isotopic composition of aerosols collected in a parking structure, *Sci. Total Environ.*, 407(18), 5104–5109, doi:10.1016/j.scitotenv.2009.05.053, 2009.

Marcus, M. A., Macdowell, A. A., Celestre, R., Manceau, A., Miller, T., Padmore, H. A. and Sublett, R. E.: Beamline 10.3.2 at ALS: a hard X-ray microprobe for environmental and materials sciences, *J. Synchrotron Radiat.*, 11, 239–247, doi:10.1107/S0909049504005837, 2004.

Marcus, M. A., Westphal, A. J. and Fakra, S. C.: Classification of Fe-bearing species from K-edge XANES data using two-parameter correlation plots, *J. Synchrotron Radiat.*, 15(5), 463–468, doi:10.1107/S0909049508018293, 2008.

May, A. A., Nguyen, N. T., Presto, A. A., Gordon, T. D., Lipsky, E. M., Karve, M., Gutierrez, A., Robertson, W. H., Zhang, M., Brandow, C., Chang, O., Chen, S., Cicero-Fernandez, P., Dinkins, L., Fuentes, M., Huang, S. M., Ling, R., Long, J., Maddox, C., Massetti, J., McCauley, E., Miguel, A., Na, K., Ong, R., Pang, Y., Rieger, P., Sax, T., Truong, T., Vo, T., Chattopadhyay, S., Maldonado, H., Maricq, M. M. and Robinson, A. L.: Gas- and particle-phase primary emissions from in-use, on-road gasoline and diesel vehicles, *Atmos. Environ.*, 88, 247–260, doi:10.1016/j.atmosenv.2014.01.046, 2014.

Moore, J. K. and Abbott, M. R.: Surface chlorophyll concentrations in relation to the Antarctic Polar Front: Seasonal and spatial patterns from satellite observations, *J. Mar. Syst.*, 37(1–3), 69–86, doi:10.1016/S0924-7963(02)00196-3, 2002.

Neyens, E. and Baeyens, J.: A review of classic Fenton's peroxidation as an advanced oxidation technique, *J. Hazard. Mater.*, 98(1–3), 33–50, doi:10.1016/S0304-3894(02)00282-0, 2003.

Norbeck, J. M., Durbin, T. D. and Truex, T. J.: Measurement of primary particulate matter emissions from light-duty motor vehicles, Riverside., 1998.

Oakes, M., Weber, R. J., Lai, B., Russell, A. and Ingall, E. D.: Characterization of iron speciation in urban and rural single particles using XANES spectroscopy and micro X-ray fluorescence measurements: Investigating the relationship between speciation and fractional iron solubility, *Atmos. Chem. Phys.*, 12(2), 745–756, doi:10.5194/acp-12-745-2012, 2012a.

Oakes, M., Ingall, E. D., Lai, B., Shafer, M. M., Hays, M. D., Liu, Z. G., Russell, A. G. and Weber, R. J.: Iron solubility related to particle sulfur content in source emission and ambient fine particles,

Environ. Sci. Technol., 46(12), 6637–6644, doi:10.1021/es300701c, 2012b.

Paris, R. and Desboeufs, K. V.: Effect of atmospheric organic complexation on iron-bearing dust solubility, *Atmos. Chem. Phys.*, 13(9), 4895–4905, doi:10.5194/acp-13-4895-2013, 2013.

Paris, R., Desboeufs, K. V. and Journet, E.: Variability of dust iron solubility in atmospheric waters: Investigation of the role of oxalate organic complexation, *Atmos. Environ.*, 45(36), 6510–6517, doi:10.1016/j.atmosenv.2011.08.068, 2011.

Park, S., Nam, H., Chung, N., Park, J.-D. and Lim, Y.: The role of iron in reactive oxygen species generation from diesel exhaust particles, *Toxicol. Vitro.*, 20(6), 851–857, doi:10.1016/j.tiv.2005.12.004, 2006.

Pehkonen, S. O., Siefert, R., Erel, Y., Webb, S. and Hoffmann, M. R.: Photoreduction of Iron Oxyhydroxides in the Presence of Important Atmospheric Organic Compounds, *Environ. Sci. Technol.*, 27(10), 2056–2062, doi:10.1021/es00047a010, 1993.

Pignatello, J. J., Oliveros, E. and MacKay, A.: Advanced oxidation processes for organic contaminant destruction based on the fenton reaction and related chemistry, *Crit. Rev. Environ. Sci. Technol.*, 36(1), 1–84, doi:10.1080/10643380500326564, 2006.

Rubio-Clemente, A., Torres-Palma, R. A. and Peñuela, G. A.: Removal of polycyclic aromatic hydrocarbons in aqueous environment by chemical treatments: A review, *Sci. Total Environ.*, 478, 201–225, doi:10.1016/j.scitotenv.2013.12.126, 2014.

Saliba, G., Saleh, R., Zhao, Y., Presto, A. A., Lambe, A. T., Frodin, B., Sardar, S., Maldonado, H., Maddox, C., May, A. A., Drozd, G. T., Goldstein, A. H., Russell, L. M., Hagen, F. and Robinson, A. L.: Comparison of Gasoline Direct-Injection (GDI) and Port Fuel Injection (PFI) Vehicle Emissions: Emission Certification Standards, Cold-Start, Secondary Organic Aerosol Formation Potential, and Potential Climate Impacts, *Environ. Sci. Technol.*, 51(11), 6542–6552,

doi:10.1021/acs.est.6b06509, 2017.

Schauer, J. J., Kleeman, M. J., Cass, G. R. and Simoneit, B. R. T.: Measurement of emissions from air pollution sources. 5. C1-C32 organic compounds from gasoline-powered motor vehicles., *Environ. Sci. Technol.*, 36(6), 1169–1180, doi:10.1021/es0108077, 2002.

Sedwick, P. N., Sholkovitz, E. R. and Church, T. M.: Impact of anthropogenic combustion emissions on the fractional solubility of aerosol iron: Evidence from the Sargasso Sea, *Geochemistry, Geophys. Geosystems*, 8(10), doi:10.1029/2007GC001586, 2007.

Shi, Z., Krom, M. D., Jickells, T. D., Bonneville, S., Carslaw, K. S., Mihalopoulos, N., Baker, A. R. and Benning, L. G.: Impacts on iron solubility in the mineral dust by processes in the source region and the atmosphere: A review, *Aeolian Res.*, 5, 21–42, doi:10.1016/j.aeolia.2012.03.001, 2012.

Sholkovitz, E. R., Sedwick, P. N. and Church, T. M.: Influence of anthropogenic combustion emissions on the deposition of soluble aerosol iron to the ocean: Empirical estimates for island sites in the North Atlantic, *Geochim. Cosmochim. Acta*, 73(14), 3981–4003, doi:10.1016/j.gca.2009.04.029, 2009.

Sholkovitz, E. R., Sedwick, P. N., Church, T. M., Baker, A. R. and Powell, C. F.: Fractional solubility of aerosol iron: Synthesis of a global-scale data set, *Geochim. Cosmochim. Acta*, 89, 173–189, doi:10.1016/j.gca.2012.04.022, 2012.

Stumm, W. and Morgan, J. J.: *Aquatic Chemistry: Chemical Equilibria and Rates in Natural Water*, 3rd ed., Wiley-Interscience., 1996.

Tagliabue, A., Bowie, A. R., Philip, W., Buck, K. N., Johnson, K. S. and Saito, M. A.: Review The integral role of iron in ocean biogeochemistry, *Nat. Publ. Gr.*, 543(7643), 51–59, doi:10.1038/nature21058, 2017.

Verma, V., Fang, T., Guo, H., King, L., Bates, J. T., Peltier, R. E., Edgerton, E., Russell, A. G. and Weber, R. J.: Reactive oxygen species associated with water-soluble PM_{2.5} in the southeastern United States: Spatiotemporal trends and source apportionment, *Atmos. Chem. Phys.*, 14(23), 12915–12930, doi:10.5194/acp-14-12915-2014, 2014.

Vile, G. F., Winterbourn, C. C. and Sutton, H. C.: Radical-driven fenton reactions: Studies with paraquat, adriamycin, and anthraquinone 6-sulfonate and citrate, ATP, ADP, and pyrophosphate iron chelates, *Arch. Biochem. Biophys.*, 259(2), 616–626, doi:10.1016/0003-9861(87)90528-5, 1987.

Wang, Y., Arellanes, C. and Paulson, S. E.: Hydrogen peroxide associated with ambient fine-mode, diesel, and biodiesel aerosol particles in Southern California, *Aerosol Sci. Technol.*, 46(4), 394–402, doi:10.1080/02786826.2011.633582, 2012.

Zhao, Y., Nguyen, N. T., Presto, A. A., Hennigan, C. J., May, A. A. and Robinson, A. L.: Intermediate Volatility Organic Compound Emissions from On-Road Diesel Vehicles: Chemical Composition, Emission Factors, and Estimated Secondary Organic Aerosol Production, *Env. Sci. Tech.*, 49, 11516–11526, doi:10.1021/acs.est.5b02841, 2015.

Zhao, Y., Nguyen, N. T., Presto, A. A., Hennigan, C. J., May, A. A. and Robinson, A. L.: Intermediate Volatility Organic Compound Emissions from On-Road Gasoline Vehicles and Small Off-Road Gasoline Engines., *Environ. Sci. Technol.*, 50, 4554–4563, doi:10.1021/acs.est.5b06247, 2016.

Zhu, X., Prospero, J. M., Savoie, D. L., Millero, F. J., Zika, R. G. and Saltzman, E. S.: Photoreduction of iron(III) in marine mineral aerosol solutions, *J. Geophys. Res. Atmos.*, 98(D5), 9039–9046, doi:10.1029/93JD00202, 1993.

Tables and Figures and Captions

Table 1: Average of total trace total and water soluble elements from car exhaust reported in EF ($\mu\text{g kg-fuel}^{-1}$). These samples represent a range of different makes and models of cars. The values in the parenthesis are the range of the vehicle populualtion. (n=32)

Table 2: Comparison of exhaust composition in g km^{-1} from different dynamometer studies which included both gasoline and diesel powered light duty vehicles. The values are the mean of the vehicle population and the values in the parenthesis are the minimum and maximum values. This table is in g km^{-1} opposed to g kg-fuel^{-1} in Table 1.

Table 1:

	Total Elements	Water-Soluble Elements
Trace elements ($\mu\text{g kg-fuel}^{-1}$)		
Na	50 (0, 200)	30 (0, 100)
Mg	40 (0, 200)	8 (0, 60)
Al	100 (0, 2000)	20 (0, 100)
K	20 (0, 100)	20 (0, 100)

Ca	200 (0, 1000)	200 (0, 1000)
Ti	1 (0, 60)	0.2 (0, 2)
V	0.02 (0, 0.7)	0.02 (0, 0.7)
Cr	5 (0.04, 20)	0.6 (0, 4)
Mn	2 (0.02, 10)	1 (0.007, 8)
Fe	80 (0, 400)	20 (0, 200)
Co	0.2 (0, 1)	0.04 (0, 0.7)
Ni	5 (0, 30)	2 (0, 10)
Cu	20 (0, 200)	20 (0, 100)
Zn	60 (0, 300)	40 (0, 300)
As	0.006 (0, 0.03)	0.006 (0, 0.03)
Se	0.3 (0, 2)	0.05 (0, 0.5)
Rb	0.2 (0, 0.5)	0.01 (0, 0.1)
Sr	1 (0.01, 4)	0.6 (0.003, 3)
Mo	5 (0, 20)	3 (0.002, 30)
Rh	0.06 (0, 0.5)	0.007 (0, 0.1)
Pd	0.8 (0, 6)	0.3 (0, 4)
Ag	0.1 (0, 2)	0.03 (0, 0.5)
Cd	0.007 (0, 0.3)	0.009 (0, 0.05)
Sb	0.2 (0, 1)	0.1 (0, 0.9)
Cs	0.005 (0, 0.02)	0.002 (0, 0.02)
Ba	5 (0, 20)	3 (0.06, 20)
Ce	4 (0, 40)	0.4 (0, 2)
Pt	0.04 (0, 0.4)	0.01 (0, 0.2)
Pb	0.4 (0, 7)	0.3 (0, 7)
U	0.002 (0, 0.03)	0.002 (0, 0.03)

Table 2:

	This study Gasoline (n = 32)	Gasoline(Schauer et al., 2002) (n=9)	Gasoline(Norbeck et al., 1998) (n=40)	Diesel(Norbeck et al., 1998) (n=19)
Fleet Age	1990-2014	1981-1994	1972-1990	1977-1993

PM components (mg km ⁻¹)				
OC	1 (0.06, 10)	3.3 ± 0.21	16 ± 32	150 ± 330
EC	10 (0.06, 100)	0.77 ± 0.023	3.5 ± 4.8	160 ± 100
sulfate	0.02 (0.001, 0.1)	0.08 ± 0.16	0.93 ± 1.9	0.77 ± .93
Trace elements (µg km ⁻¹)				
Ag	0.01 (0, 0.25)	4.5 ± 20	0	0
Al	10 (0, 110)	20 ± 17	19 ± 37	31 ± 75
Ba	0.6 (0, 4.4)	0	0	68 ± 75
Ca	30 (0, 130)	26 ± 8.5	81 ± 120	650 ± 930
Cd	0.00 (0, 0.04)	0	0	0
Co	0.01 (0,0.25)	-	0	0
Cr	0.6 (0.008, 4)	0	0	6.2 ± 12
Cu	3 (0, 27)	0	6.2 ± 6.2	19 ± 31
Fe	10 (0, 62)	8.3 ± 2.3	280 ± 680	830 ± 1000
K	2 (0, 15)	3.0 ± 11.3	0	50 ± 170
Mg	7 (0, 120)	-	25 ± 31	99 ± 200
Mn	0.2 (0.002, 1.3)	0	0	6.2 ± 6.2
Mo	0.5 (0, 3.6)	2.3 ± 6.8	0	6.2 ± 12
Ni	0.6 (0, 5.2)	0	6.2 ± 12	12 ± 18
Pb	0.04 (0, 0.57)	0	25 ± 93	19 ± 62
Sb	0.02 (0, 0.21)	17 ± 39	0	0
Sr	0.1 (0, 0.68)	0.75 ± 2.3	0	0
Zn	7 (0, 37)	14 ± 1.5	110 ± 170	810 ± 1500